Inorg. Chem. **2009**, *48*, 4536−4541

Spin Frustration and Long-Range Ordering in an AlB_2-like Metal-Organic Framework with Unprecedented N,N,N-Tris-tetrazol-5-yl-amine Ligand

Xian-Ming Zhang,*,† Tao Jiang,† Hai-Shun Wu,† and Ming-Hua Zeng‡

School of Chemistry & Material Science, Shanxi Normal University, Linfen 041004, P. R. China, and Department of Chemistry and Chemical Engineering, Guangxi Normal University, Guilin 541004, P. R. China

Received February 12, 2009

Solvothermal treatment of a mixture of $Co(OAc)_2$, NaN_3, $NaN(CN)_2$, HF, MeCN, and H_2O generated an AlB_2-like metal-organic framework, namely, $[\{(Co_3F)_3(trta)_2(H_2O)_9\}\{Co(Hbta)_3\}_2]\cdot 11H_2O$ (**1**) (H_3trta = N,N,N-tris-tetrazol-5-yl-amine; H_3bta = N,N-bis-tetrazol-5-yl-amine), in which supertrianglar supramolecular building blocks (SBBs) $\{(Co_3F)_3(trta)_2\}$ act as 12-connected nodes of hexagonal prisms. The unprecedented ligand N,N,N-tris-tetrazol-5-yl-amine is in situ generated via metal-assisted reactions of $NaN(CN)_2$, MeCN, and NaN_3, and a possible mechanism involves both 1,3-dipolar cycloaddition and nucleophilic addition. The F-centered Co_3 triangles are bridged by trta groups to result in supertriangular $\{(Co_3F)_3(trta)_2\}$ SBBs that are further arranged in a frustrated triangular lattice. The long-range ordering temperature is reduced to 4.8 K due to strong spin frustration.

Introduction

Antiferromagnets based on triangular or Kagome lattices have received much attention from both theoretical and experimental points of view because magnetic long-range ordering may be suppressed or significantly reduced as a result of inherent spin frustration that occurs when the structural arrangement of spins precludes the simultaneous satisfaction of all nearest-neighbor interactions.[1,2] Experimentally, however, only a few candidates for geometrical frustration in two dimensions have been reported. Thus, the preparation of new geometrically spin-frustrated magnetic materials that approximate theoretical models is a challenge. Topological development in metal-organic frameworks amplifies the context of geometrical frustration.[3] The (6,12)-connected AlB_2 structure is one of the most important structural types in intermetallic compounds and can be viewed as alternate packing of triangular Al and honeycomb B sheets.[4] The coordination figures of Al and B centers in AlB_2 are a hexagonal prism and a trigonal prism, respectively. Metal-organic replication of an AlB_2-like network is very important from both topological and magnetic points of view: (1) the local connectivity number in an AlB_2 network is as high as 12, which is rare in metal-organic frameworks;[5] (2) if the 12-connected nodes are spin-carrying metal ions, metal clusters, or supramolecular building blocks (SBBs), the AlB_2 topological metal-organic frameworks would be good models for the study of spin frustration due

* To whom correspondence should be addressed. Tel. & Fax: +86 357 2051402. E-mail: zhangxm@dns.sxnu.edu.cn.
† Shanxi Normal University.
‡ Guangxi Normal University.

(1) (a) Nakatsuji, S.; Nambu, Y.; Tonomura, H.; Sakai, O.; Jonas, S.; Broholm, C.; Tsunetsugu, H.; Qiu, Y.; Maeno, Y. *Science* **2005**, *309*, 1697. (b) Lee, S. H.; Broholm, C.; Ratcliff, C.; Gasparovic, G.; Huang, Q.; Kim, T. H.; Cheong, S. W. *Nature (London)* **2002**, *418*, 856.
(2) (a) Humphrey, S. M.; Wood, P. T. *J. Am. Chem. Soc.* **2004**, *126*, 13236. (b) Nytko, E. A.; Helton, J. S.; Muller, P.; Nocera, D. G. *J. Am. Chem. Soc.* **2008**, *130*, 2922. (c) Zheng, Y.-Z.; Tong, M.-L.; Xue, W.; Zhang, W.-X.; Chen, X.-M.; Grandjean, F.; Long, G. J. *Angew. Chem., Int. Ed.* **2007**, *46*, 6076.
(3) (a) Yaghi, O. M.; O'Keeffe, M.; Ockwig, N. W.; Chae, H. K.; Eddadoudi, M.; Kim, J. *Nature (London)* **2003**, *423*, 705. (b) Férey, G.; Mellot-Draznieks, C.; Serre, C.; Millange, F. *Acc. Chem. Res.* **2005**, *38*, 217. (c) Ockwig, N. W.; Delgado-Friedrichs, O.; O'Keeffe, M.; Yaghi, O. M. *Acc. Chem. Res.* **2005**, *38*, 176. (d) Bradshaw, D.; Claridge, J. B.; Cussen, E. J.; Prior, T. J.; Rosseinsky, M. J. *Acc. Chem. Res.* **2005**, *38*, 273. (e) Kitagawa, S.; Kitaura, R.; Noro, S. *Angew. Chem. Int. Ed.* **2004**, *43*, 2334. (f) Rao, C. N. R.; Natarajan, S.; Vaidhyanathan, R. *Angew. Chem., Int. Ed.* **2004**, *43*, 1466.
(4) Delgado-Friedrichs, O.; O'Keeffe, M.; Yaghi, O. M. *Acta Crystallogr.* **2006**, *A62*, 350–355.
(5) (a) Zhang, X.-M.; Fang, R.-Q.; Wu, H.-S. *J. Am. Chem. Soc.* **2005**, *127*, 7670. (b) Li, D.; Wu, T.; Zhou, X.-P.; Zhou, R.; Huang, X.-C. *Angew. Chem., Int. Ed.* **2005**, *44*, 4175. (c) Wang, X.-L.; Qin, C.; Wang, E.-B.; Su, Z.-M.; Li, Y.-G.; Xu, L. *Angew. Chem., Int. Ed.* **2006**, *45*, 7411. (d) Jia, J.; Lin, X.; Wilson, C.; Blake, A. J.; Champness, N. R.; Hubberstey, P.; Walker, G.; Cussen, E. J.; Schröder, M. *Chem. Commun.* **2007**, 840. (e) Hao, Z.-M.; Fang, R.-Q.; Wu, H.-S.; Zhang, X.-M. *Inorg. Chem.* **2008**, *47*, 8197. (f) Hill, R. J.; Long, D.-L.; Champness, N. R.; Hubberstey, P.; Schröder, M. *Acc. Chem. Res.* **2005**, *38*, 337.

10.1021/ic9002912 CCC: $40.75
Published on Web 04/06/2009

to the inherent triangular lattice of 12-connected nodes in AlB_2. Because the cuboctahedron rather than the hexagonal prism is the preferred geometric figure of stereochemically unconstrained 12-coordination, the supramolecular building block approach[6] has been used herein to construct AlB_2-like metal-organic frameworks.

On the other hand, in situ syntheses of novel ligands in the crystal engineering of complexes are of great interest in coordination chemistry for the discovery of new metal-assisted organic reactions and understanding their mechanisms.[7] Organonitriles usually do not behave as either strong σ donors or effective π-electron acceptors, which are of major importance in both the laboratory and industry because nucleophilic or electrophilic addition or 1,3-dipolar cycloaddition to the C≡N triple bond offers an attractive route for the creation of novel C−C, C−N, C−O, and C−S bonds.[8−12] However, due to insufficient reactivity of the nitriles, most of the above reactions usually require activation of the RCN by ligation to a metal center, which provides more convenient methods than conventional processes.[8] The tetrazolyl functional group has found a wide range of applications in coordination chemistry, pharmaceuticals, photography, information recording systems, and high-density energy materials.[13] In 2001, Sharpless reported an environmentally friendly process for the preparation of 5-substituted 1H-tetrazoles via metal-assisted 1,3-dipolar cycloaddition of nitriles and azide,[14] and Xiong and others subsequently developed a series of coordination polymers with in situ synthesized tetrazoles with this method.[11,15,16] However, in situ synthesis of a novel tetrazolyl ligand that involves both 1,3-dipolar cycloaddition and nucleophilic addition has not been documented.

In our ongoing investigation of high-connected metal-organic frameworks and in situ ligand reactions,[5a,7c] solvothermal treatment of a mixture of $Co(OAc)_2$, NaN_3, $NaN(CN)_2$, HF, MeCN, and H_2O at 180 °C for 98 h generated a (6,12)-connected AlB_2 topological metal-organic framework, namely, $[\{(Co_3F)_3(trta)_2(H_2O)_9\}\{Co(Hbta)_3\}_2]\cdot 11H_2O$ (**1**) (H_3trta = N,N,N-tris-tetrazol-5-yl-amine; H_3bta = N,N-bis-tetrazol-5-yl-amine), in which SBBs $\{Co(Hbta)_3\}$ and $\{(Co_3F)_3(trta)_2(H_2O)_9\}$ act as six-connected nodes of a trigonal prism and 12-connected nodes of a hexagonal prism, respectively.

Experimental Section

General Remarks. The FT-IR spectra were recorded from KBr pellets in the range 400−4000 cm^{-1} on a Nicolet 5DX spectrometer. Elemental analyses were performed on a Perkin-Elmer 240 elemental analyzer. Thermal analyses were carried out in the air using SETARAM LABSYS equipment with a heating rate of 10 °C/min, which show a single weight loss of 65.8% in the temperature range of 180−550 °C (Figure S1, Supporting Information). The magnetic measurements were performed with Quantum Design SQUID MPMS XL-5 instruments. The diamagnetism of the sample and holder were taken into account. ESI-MS spectra were performed on a Thermo Finigan LCQ DECA XP quadrupole ion trap mass spectrometer using an electrospray ionization source with methanol as the mobile phase. All spectra were acquired in the positive ion mode, and the spray voltage was set at 4500 V.

Syntheses. Synthesis of $[\{(Co_3F)_3(trta)_2(H_2O)_9\}\{Co(Hbta)_3\}_2]\cdot 11H_2O$ (1). A mixture of $Co(Oac)_2$ (0.4 mmol, 0.100 g), NaN_3 (0.6 mmol, 0.039 g), $NaN(CN)_2$ (0.2 mmol, 0.027 g), MeCN (2 mL), and H_2O (5 mL) in a molar ratio of 1:1:5:0.5:690:94 was stirred and adjusted by hydrofluoric acid to a pH of ca. 2 and then sealed in a 15-mL Teflon-lined stainless container and heated to 180 °C for 98 h. After it was cooled to room temperature and subjected to filtration, red block crystals of **1** in 35% yield were recovered. Anal. calcd for $C_{18}H_{46}Co_{11}F_3N_{80}O_{20}$ (**1**): C, 8.91; H, 1.99; N, 46.18. Found: C, 8.72; H, 2.12; N, 45.90. IR (KBr, cm^{-1}): 3356sb, 2924w, 2364m, 2344w, 1619s, 1549w, 1490w, 1446m, 1266s, 1163m, 1134s, 1030s, 858m, 806s, 745s, 713w, 604m.

X-Ray Crystallography. Data were collected at 298 K on a Bruker Apex diffractometer (Mo Kα, λ = 0.71073 Å). Lorentz-polarization and absorption corrections were applied. The structure was solved with direct methods and refined with full-matrix least-squares techniques (SHELX-97).[17] Analytical expressions of neutral-atom scattering factors were employed, and anomalous dispersion corrections were incorporated. All non-hydrogen atoms were refined anisotropically. The crystallographic data are listed in Table 1.

Results and Discussions

Description of Structures. X-ray diffraction reveals that **1** crystallizes in hexagonal space group $P6_3/mcm$, and the asymmetric unit consists of three crystallographically independent Co ions, one μ_3-F, 1/2 Hbta, 1/6 trta, and two coordinated water molecules (Figure 1a). The Co(1) and

(6) (a) Cairns, A. J.; Perman, J. A.; Wojtas, L.; Kravtsov, V. Ch.; Alkordi, M. H.; Eddaoudi, M.; Zaworotko, M. J. *J. Am. Chem. Soc.* **2008**, *130*, 1560. (b) Nouar, F.; Eubank, J. F.; Bousquet, T.; Wojtas, L.; Zaworotko, M. J.; Eddaoudi, M. *J. Am. Chem. Soc.* **2008**, *130*, 1833.
(7) (a) Constable, E. C. *Metals and Ligand Reactivity*; VCH: Weinheim, Germany, 1996. (b) Chen, X.-M.; Tong, M.-L. *Acc. Chem. Res.* **2007**, *40*, 162. (c) Zhang, X.-M. *Coord. Chem. Rev.* **2005**, *249*, 1201.
(8) Pombeiro, A. J. L.; Kukushkin, V. Yu. Reactivity of Coordinated Nitriles. In *Comprehensive Coordination Chemistry II*; McCleverty, J. A., Meyer, T. J., Eds.; Elsevier, Pergamon: Oxford, U.K., 2003, Vol. 1; Chapter 1.34, p 639.
(9) Kukushkin, V. Y.; Pombeiro, A. J. L. *Chem. Rev.* **2002**, *102*, 1771.
(10) Murahashi, S.-I.; Takaya, H. *Acc. Chem. Res.* **2000**, *33*, 225.
(11) Zhao, H.; Qu, Z.-R.; Ye, H.-Y.; Xiong, R.-G. *Chem. Soc. Rev.* **2008**, *37*, 84.
(12) (a) Bochkarev, M. N.; Khoroshenkov, G. V.; Schumann, H.; Dechert, S. *J. Am. Chem. Soc.* **2003**, *125*, 2894. (b) Feng, S. G.; White, P. S.; Templeton, J. L. *J. Am. Chem. Soc.* **1994**, *116*, 8613. (c) Longato, B.; Montagner, D.; Bandoli, G.; Zangrando, E. *Inorg. Chem.* **2006**, *45*, 1805.
(13) (a) Singh, H.; Chawla, A. S.; Kapoor, V. K.; Paul, D.; Malhotra, R. K. *Prog. Med. Chem.* **1980**, *17*, 151. (b) Ostrovskii, V. A.; Pevzner, M. S.; Kofmna, T. P.; Shcherbinin, M. B.; Tselinskii, I. V. *Targets Heterocycl. Syst.* **1999**, *3*, 467. (c) Hiskey, M.; Chavez, D. E.; Naud, D. L.; Son, S. F.; Berghout, H. L.; Bome, C. A. *Proc. Int. Pyrotech. Semin.* **2000**, *27*, 3.
(14) Demko, Z. P.; Sharpless, K. B. *J. Org. Chem.* **2001**, *66*, 7945.
(15) (a) Xiong, R.-G.; Xue, X.; Zhao, H.; You, X.-Z.; Abrahams, B. F.; Xue, Z.-L. *Angew. Chem., Int. Ed.* **2002**, *41*, 3800. (b) Ye, Q.; Song, Y.-M.; Wang, G.-X.; Chen, K.; Fu, D.-W.; Hong Chan, P. W.; Zhu, J.-S.; Huang, S. D.; Xiong, R.-G. *J. Am. Chem. Soc.* **2006**, *128*, 6554.
(16) (a) Gao, E.-Q.; Liu, N.; Cheng, A.-L.; Gao, S. *Chem. Commun.* **2007**, 2470. (b) Li, J.-R.; Tao, Y.; Yu, Q.; Bu, X.-H. *Chem. Commun.* **2007**, 1527. (c) Dinca, M.; Yu, A. F.; Long, J. R. *J. Am. Chem. Soc.* **2006**, *128*, 8904. (d) Wu, T.; Yi, B.-H.; Li, D. *Inorg. Chem.* **2005**, *44*, 4130. (e) Lu, Y.-B.; Wang, M.-S.; Zhou, W.-W.; Xu, G.; Guo, G.-C.; Huang, J.-S. *Inorg. Chem.* **2008**, *47*, 8935.
(17) Sheldrick, G. M. *SHELXTL-97*; University of Göttingen: Göttingen, Germany, 1997.

Table 1. Crystallographic Data for Compound **1**

formula	$C_{18}H_{46}Co_{11}F_3N_{80}O_{20}$
Mr	2408.58
cryst syst	hexagonal
space group	$P6_3/mcm$
a (Å)	15.1252(5)
b (Å)	15.1252(5)
c (Å)	17.2416(11)
α (deg)	90
β (deg)	90
γ (deg)	120
V (Å^3)	3415.9(3)
Z	2
ρ_{calcd} (g cm^{-3})	2.342
μ (mm^{-1})	2.735
F(000)	2296
size (mm)	0.21 × 0.20 × 0.20
θ (deg)	1.55 to 27.00
Measured data	18245
Unique data	1378
T_{max}/T_{min}	0.6107/0.5974
obsd data	1280
restraints	3
params	112
S	1.128
R_1[a]	0.0522
wR_2[b]	0.1603
$\Delta\rho_{max}/\Delta\rho_{min}$ (e A^{-3})	1.245/−0.914

[a] $R_1 = \sum ||F_o| - |F_c||/\sum |F_o|$. [b] $wR_2 = [\sum w(F_o^2 - F_c^2)^2/\sum w(F_o^2)^2]^{1/2}$.

Co(2) have similar octahedral coordination geometries, each ligated by four nitrogen atoms in the equatorial plane and one μ_3-F and one water molecule at the axial positions. The Co(3) center has 3.2 symmetry (Wyckoff letter: 4d), chelated by six nitrogen atoms from three Hbta groups. The doubly deprotonated Hbta adopts the μ_5-η^2:η^1:η^1:η^1:η^1 mode, while the triply deprotonated trta coordinates in the μ_3-η^2:η^2:η^2 mode. The Co(1)−F(1) and Co(2)−F(1) bond lengths are 2.050(5) and 2.133(2) Å, respectively. Two Co(2)'s and one Co(1) are bridged by a μ_3-F to generate a F-centered Co_3, an isosceles triangle. Within an F-centered Co_3 triangle, Co(1)···Co(2) and Co(2)···Co(2) distances are 3.438 and 3.996 Å, and Co(1)−F−Co(2) and Co(2)−F−Co(2) angles are 110.50(13) and 139.0(3)°, respectively. Three Co_3F clusters are bridged by two trta groups to result in a supertriangular SSB $\{(Co_3F)_3(trta)_2\}$ with D_{3h} symmetry (Figure S3, Supporting Information). The second SSB is $\{Co(Hbta)_3\}$ with D_3 symmetry. Each $\{Co(Hbta)_3\}$ SSB is connected to six $\{(Co_3F)_3(trta)_2(H_2O)_9\}$ SSBs, while each $\{(Co_3F)_3(trta)_2(H_2O)_9\}$ SSB is connected to 12 $\{Co(Hbta)_3\}$ SSBs (Figure 1b and c). The structure of **1** can be described as an augmented (6,12)-connected AlB_2-like 3D network in which the SSBs $\{Co(Hbta)_3\}$ and $\{(Co_3F)_3(trta)_2(H_2O)_9\}$ act as six-connected nodes of a trigonal prism and 12-connected nodes of a hexagonal prism, respectively (Figure 1d and Scheme 1). The short *Schläfli* symbol for **1** is $\{4^{15}\}_2\{4^{48}\cdot 6^{18}\}$.[18] Alternately, **1** is constructed by two types of alternately arranged supramolecular sheets: a triangular sheet consisting of $\{(Co_3F)_3(trta)_2(H_2O)_9\}$ SBBs (Figure 2) and a honeycomb sheet consisting of $\{Co(Hbta)_3\}$ SBBs (Figure S4, Supporting Information). Each unit cell is composed of two triangular sheets and two honeycomb sheets. Only six lattice water molecules in the formula can be located from the Fourier map, and the additional five lattice water molecules are deduced by elemental analysis and thermogravimetric analysis. The existence of additional lattice water molecules are also in agreement with the calculation by PLATON,[19] which shows that the potential solvent area volume is 365.5 Å^3 per unit cell volume.

The most interesting structural feature of **1** is in situ formation of unprecedented trta and documented Hbta, two types of tetrazolyl ligands. The trta trianion shows symmetry of 3.m (Wyckoff letter: 4e) with an approximate planar configuration, and the central N(8) atom is bonded to three equivalent C(2) atoms with a N(8)−C(2) distance of 1.439(12) Å. All C(2)−N(8)−C(2j), C(2)−N(8)−C(2k), and C(2j)−N(8)−C(2k) angles are 119.5(2)° (Figure 1a). Each tetrazolyl group in the trta trianion shows two long C(2)−N(6) and C(2)−C(6i) bonds of 1.429(9) Å, one middle N(7)−N(7i) bond of 1.349(15) Å, and two short N(6)−N(7) and N(6i)−N(7i) bonds of 1.265(9) Å, indicating that two double bonds of a tetrazolyl in trta are mainly located between N(6) and N(7) atoms and three negative charges of the trta trianion are mainly located at the three C(2) carbon atoms. Besides the X-ray single-crystal structure, evidence for in situ synthesis of the trta trianion also comes from ESI-MS. Single crystals of **1** were decomposed by hydrochloric acid, and the resulting mixture was extracted with methanol for ESI measurement (Figure 3). The ESI-MS spectrum in positive mode obviously shows a signal at *m*/*z* 222.0, corresponding to protonated N,N,N-tris-tetrazol-5-yl-amine. The signal at *m*/*z* 154.0 is in agreement with protonated N,N-bis-tetrazol-5-yl-amine. It has been documented that N,N-bis-tetrazol-5-yl-amine can in situ generate via the direct 1,3-dipolar cycloaddition of $NaN(CN)_2$ and azide.[16] In situ formation of N,N,N-tris-tetrazol-5-yl-amine is unprecedented and very difficult. In order to get insight into the mechanism, comparative experiments were carried out, which showed that **1** was only available in the presence of MeCN. Although an exact mechanism is unclear at present, the main steps for the trta trianion are proposed based on comparative experiments and common knowledge of nitriles (Scheme 2). First, a MeCN is coordinated to a Co(II) ion, which results in nucleophilic activation of MeCN. Second, nucleophilic addition by $HN(CN)_2$ to coordinated MeCN gives an amidine species. Third, elimination of methane from amidine gives tricyanamide. Finally, the 1,3-dipolar cycloaddition reaction of tricyanamide and azide finishes the trta species. The crystalline carbon(IV) nitride phase is speculated to be harder than diamond, and one way to acquire this material is through high-pressure transformation of a molecule with C_3N_4 stoichiometry.[20] The tricyanamide represents the smallest molecular carbon(IV) nitride, which has not been isolated to date.

Magnetic Properties. The temperature dependence of the magnetic susceptibility for **1** in the temperature range 2−300 K under a 2000 Oe applied field was studied with a Quantum Design SQUID MPMS XL-5 (Figure 4). In the paramagnetic

(18) Blatov, V. A. *TOPOS*; Samara State University: Russia, 2004.

(19) Spek, A. L. *PLATON*; Utrecht University: Utrecht, The Netherlands, 1999.

(20) Kroke, E.; Schwarz, M. *Coord. Chem. Rev.* **2004**, *248*, 493.

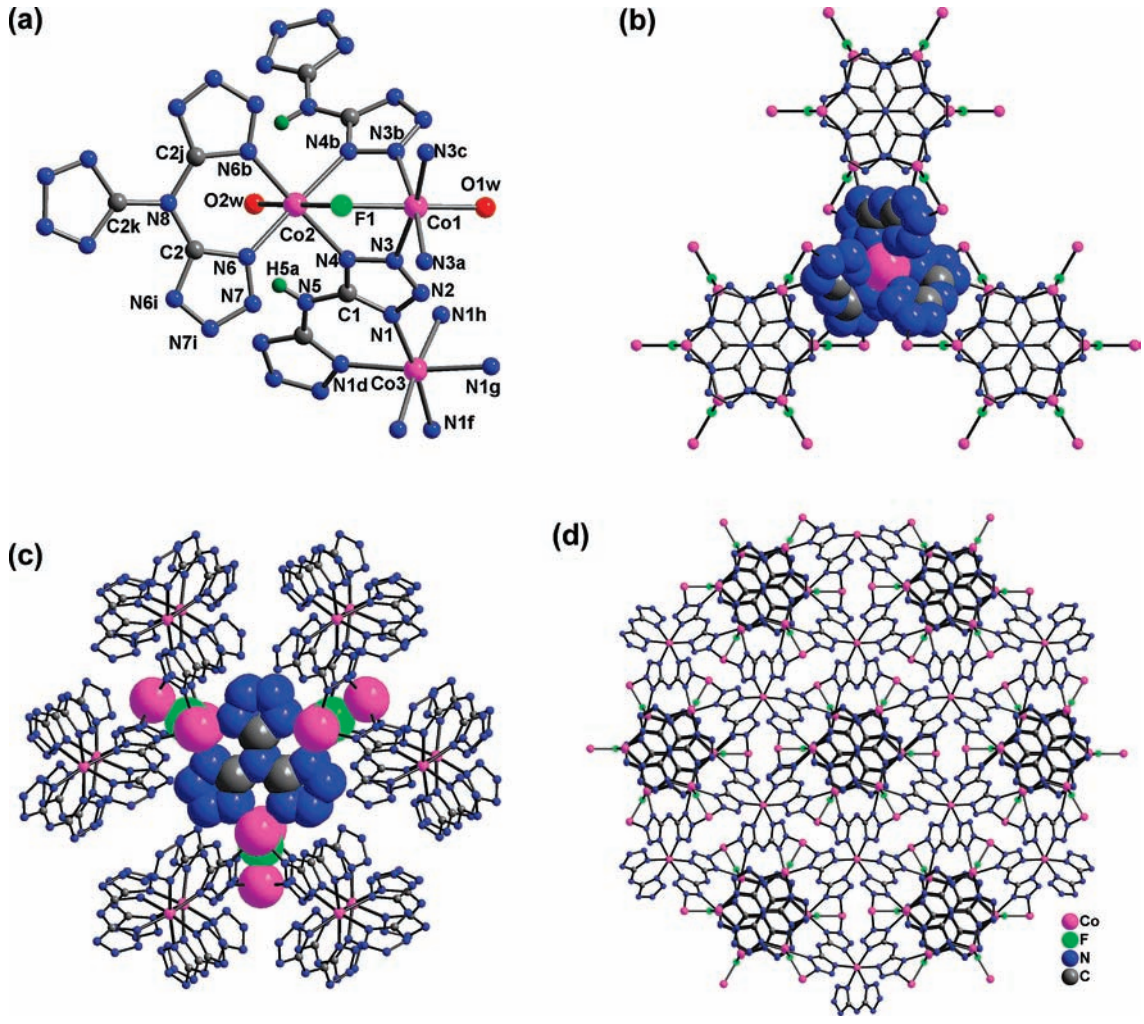

Figure 1. (a) View of the coordination environments of Co atoms, (b) each {Co(Hbta)$_3$} SBB connected to six {(Co$_3$F)$_3$(trta)$_2$(H$_2$O)$_9$} SBBs, (c) each {(Co$_3$F)$_3$(trta)$_2$} SBB connected to 12 {Co(Hbta)$_3$} SBBs, and (d) a 3-D AlB$_2$-like network in **1**.

Scheme 1. Schematic View of an Augmented AlB$_2$-like Net[a]

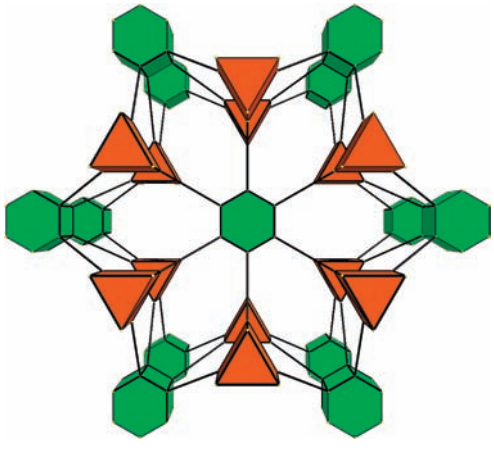

[a] Green hexagonal prisms and brown trigonal prisms represent {(Co$_3$F)$_3$(trta)$_2$} and {Co(Hbta)$_3$} SBBs, respectively.

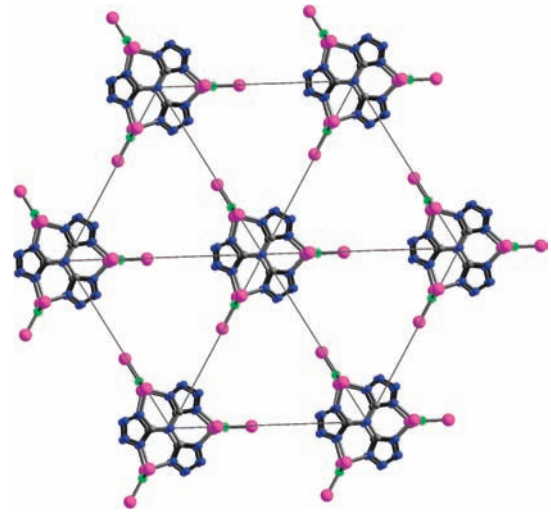

Figure 2. View of triangular supramolecular sheet of {(Co$_3$F)$_3$(trta)$_2$}.

region above 50 K, the fitting of Curie−Weiss law gives a Curie constant $C = 37.99$ cm^3 K mol^{-1} and a Weiss constant $\theta = -60.2$ K. The Curie constant C corresponds to an effective moment of 5.25 μ_B per Co(II) ion, within the range for an orbital contributed high-spin octahedral Co(II) system.[21] The $\chi_m T$ value at 300 K is 30.61 cm^3 K mol^{-1} per Co_{11} unit and slowly decreases with lowering temperature down to a minimum value of 5.53 cm^3 K mol^{-1} at 7 K. Upon further cooling, the $\chi_m T$ value increases to a maximum of 19.26 cm^3 K mol^{-1} at 4 K and then decreases to 14.53 cm^3 K mol^{-1} at 2 K. The increase of the $\chi_m T$ value at low temperatures is probably due to odd Co(II) centers or spin-

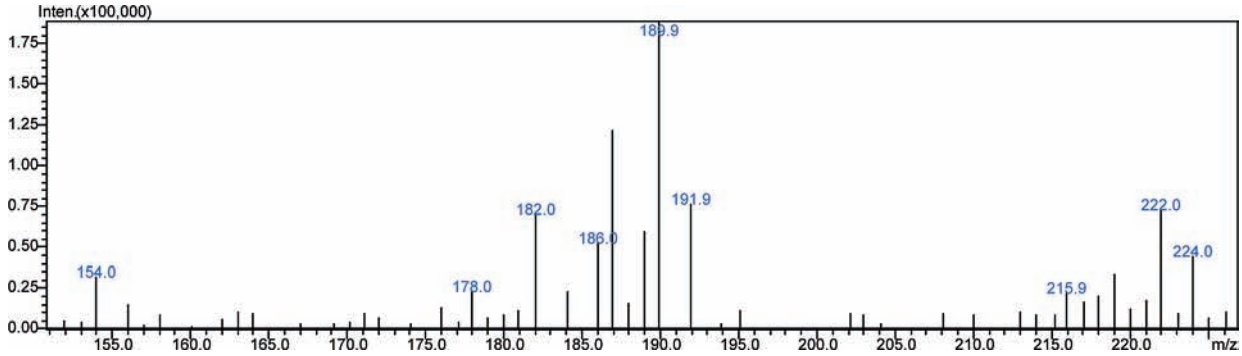

Figure 3. ESI-MS for hydrochloric acid decomposed **1**.

Scheme 2. Possible Mechanism for N,N,N-Tris-tetrazol-5-yl-amine from $NaN(CN)_2$, MeCN, and NaN_3

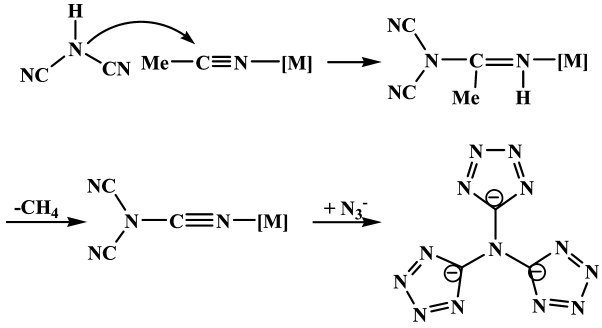

canting behavior.[2c] It is worth noting that a minor discontinuity around 50 K is observed, which generally comes from magnetic phase transition or a minor impurity. Field-cooled magnetizations in different applied dc fields clearly show an abrupt increase below 5 K, which is an indication of the onset of magnetic ordering (Figure 5). Both real χ' and imaginary χ'' components are present at $T_N = 4.8$ K in ac susceptibilities, and no frequency dependence indicates 3D long-range ordering of a canted antiferromagnet (Figure 6). The magnetization curve is also characteristic of a canted antiferromagnet, and the hysteresis loop at 2 K is observed with a coercive field of 75 Oe and a remnant magnetization of 0.45 Nβ (Figure 7). Ramirez has provided a measure for spin frustration by defining $f = |\theta|/T_N$, with an f value above 10 signifying a strong frustration.[22] From the above θ value of -60.2 K and the T_N value of 4.8 K, an f value of 12.5 is obtained for **1**, which indicates the presence of strong spin frustration and can be understood from the below three levels.

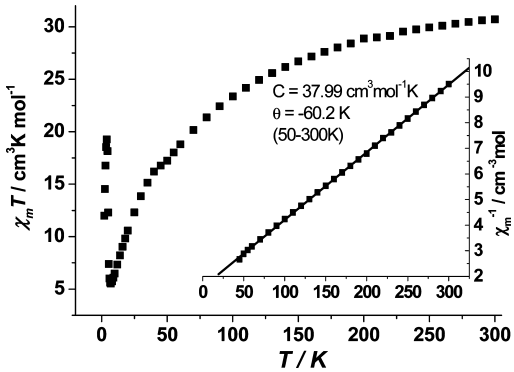

Figure 4. The $\chi_m T$ versus T curve at a field of 2000 Oe per Co_{11} unit in **1**. Inset: Curie−Weiss fitting of the $1/\chi_m$ versus T curve.

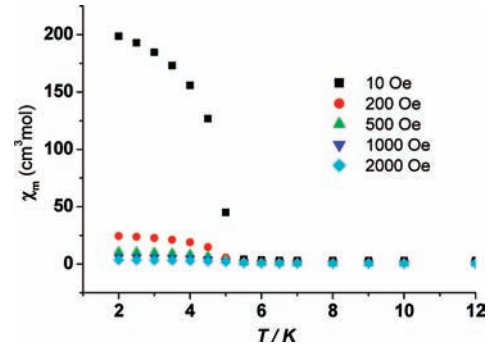

Figure 5. Field-cooled (FC) magnetic susceptibility.

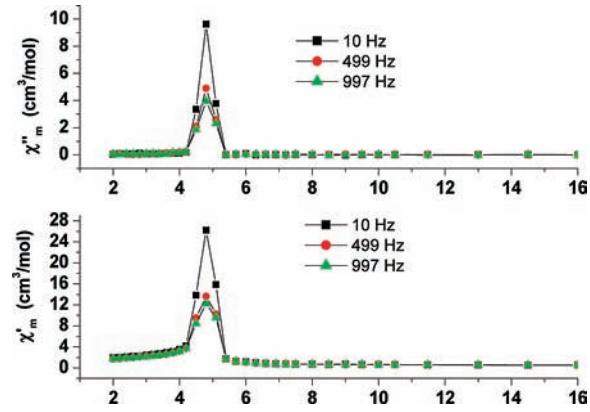

Figure 6. The ac magnetic susceptibility of real and imaginary components measured under $H_{dc} = 0$ Oe and $H_{ac} = 1$ Oe applied fields.

Within an F-cetered Co_3 isosceles triangle, strong antiferromagnetic Co···Co interactions induce spin competition. Within a supertrianglar SBB $\{(Co_3F)_3(trta)_2\}$, three F-centered Co_3 isosceles triangles are geometrically frustrated; within a supramolecular triangular sheet, the supertrianglar SBBs $\{(Co_3F)_3(trta)_2\}$ are geometrically frustrated. To note, **1** has some limitation as an ideal geometrically frustrated triangular lattice. This is because of the presence of weak three-atom-bridge Co···Co superexchange interactions between $\{(Co_3F)_3(trta)_2\}$ and $\{Co(Hbta)_3\}$ SBBs. The Co(3) of $\{Co(Hbta)_3\}$ SBB is weakly interacted with six Co(1) and six Co(2) ions from $\{(Co_3F)_3(trta)_2\}$ SBBs. However, the 12 Co ions around the Co(3) ion are arranged into four equilateral triangles, which possibly has some contribution

(21) Casey, A. T.; Mitra, S. Magnetic Behavior of Compounds Containing d^n Ions. In *Theory and Applications of Molecular Paramagnetism*; Boudreaux, E. A., Mulay, L. N., Eds.; John Wiley & Sons: New York, 1976; p 198.

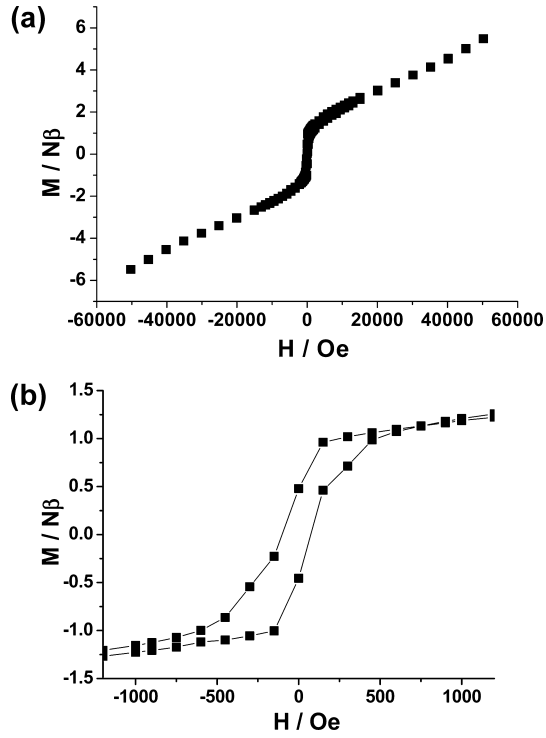

Figure 7. *M* versus *H* curve (a) and magnetic hysteresis loop (b) of **1** per Co_{11} unit measured at 2 K.

to the strong spin frustration (Figure S5, Supporting Information). As a result of spin frustration, magnetic long-range ordering is reduced to 4.8 K. It should be noted that spin frustration is also observed in $[Mn\{Mn_3(\mu_3\text{-}F)(Hbta)_3(H_2O)_6\}_2]$,[16a] which shows a 2D frustrated lattice constructed by F-centered Mn_3 triangles and mononuclear Mn(II) ions and has an *f* value of 8.8. Neither spin canting nor a hysteresis loop is observed in this Mn compound.

(22) Schiffer, P.; Ramirez, A. P. *Comments Condens. Matter Phys.* **1996**, *18*, 21.

Conclusion

A solvothermal reaction generated an AlB_2-like metal-organic framework in which supertrianglar SBBs $\{(Co_3F)_3(trta)_2\}$ and $\{Co(Hbta)_3\}$ act as 12-connected nodes of a hexagonal prism and six-connected nodes of a trigonal prism, respectively. The unprecedented ligand N,N,N-tris-tetrazol-5-yl-amine is in situ generated from $NaN(CN)_2$, MeCN, and NaN_3 via both 1,3-dipolar cycloaddition and nucleophilic addition. The F-centered Co_3 triangles are bridged by trta groups to result in supertrianglar $\{(Co_3F)_3(trta)_2\}$ SBBs that are further arranged in a frustrated triangular lattice. According to Ramirez's formula $f = |\theta|/T_N$, an *f* value of 12.5 for the titled compound indicates the presence of strong spin frustration, which can be understood from the below three levels: an isosceles triangular arrangement of three Co's within an F-centered Co_3, a geometrically frustrated arrangement of three F-centered Co_3 isosceles triangles within a supertrianglar SBB $\{(Co_3F)_3(trta)_2\}$, and a triangular lattice of supertrianglar SBBs $\{(Co_3F)_3(trta)_2\}$. The long-range ordering temperature is reduced to 4.8 K due to strong spin frustration. Strong spin frustration and long-range ordering are observed in the title compound.

Acknowledgment. This work was financially supported by NSFC (20771069) and FANEDD (200422).

Supporting Information Available: Crystal structural data for **1** and additional figures. This material is available free of charge via the Internet at http://pubs.acs.org.

IC9002912